Desalination and Water Treatment
www.deswater.com
doi: 10.5004/dwt.2021.26824

217 (2021) 159–173
March

Application of coagulation and full-membrane process in municipal reclaimed water in northern China: an optimized process

Zhao Li[a,*], Changhai Li[a], Yingqi Meng[a], Jinghui Gao[a], Hui Zhao[a], Chenlu Ye[b], Yunfei Guo[a]

[a]*Xi'an Thermal Power Research Institute Co., Ltd., Block A, Boyuan Science and Technology Building, No. 99,Yanxiang Road, Xi'an, Shaanxi 710054, P.R. China, Tel. +86 02982002616; email: lizhao1@tpri.com.cn (Z. Li), Tel. +86 02962226070; email: lichanghai@tpri.com.cn (C.H. Li), Tel. +86 02982002606; email: mengyingqi@tpri.com.cn (Y.Q. Meng), Tel. +86 02982002608; email: gaojinghui@tpri.com.cn (J.H. Gao), Tel. +86 02982002620; email: zhaohui@tpri.com.cn (H. Zhao), Tel. +86 02982002615; email: guoyunfei@tpri.com.cn (Y.F. Guo)*
[b]*Xi'an Jiaotong University, Xianning West Road, Xi'an, Shaanxi 710049, P.R. China, Tel. +86 02982668843; email: yechenlu@xjtu.edu.cn*

Received 9 July 2020; Accepted 20 November 2020

ABSTRACT

Lime coagulation and the full-membrane process are sharply being used in wastewater treatment as the technology is cost-effective. This paper studies the water treatment system in thermal power plants located in northern China. The municipal reclaimed water is processed by lime coagulation and full-membrane technique and it is the main water supply source of this power plant. An analysis is established to affirm the operation status of lime coagulation and full-membrane systems. The response surface Box–Behnken central composite design method was used to optimize the lime coagulation system to achieve the desired results. The optimal conditions are obtained by the response surface method and combine with the actual situation. In conclude, the polymerized ferrous sulfate (PFS) dosage (30 mg/L), the NaClO dosage (4.5 mg/L), the stirring rate (300 rpm), temperature (20°C), pH of flocculant area adjusted by adding calcium hydroxide (10.1), inlet flow (800 t/h) and pH of effluent adjusted by adding H_2SO_4 (6.5). Under these conditions, chemical oxygen demand and NH_3–N removal rate is 84.72%, 88.25%, and 87.74%, respectively. After the effluent passes through DMF, ultrafiltration, primary, and secondary reverse osmosis, and EDI, the effluent finally meets the requirements of high-purity water in the thermal power plants. Any problems associated with the process and solutions of corresponding problems are also discussed in this paper. All the requirements desired from lime coagulation and full-membrane technique are successfully achieved and save a large amount of freshwater resources. The annual savings for the thermal power plant is about 7.63 million USD and also there is no acid–base wastewater drainage that needs to be treated. The payback period of the project investment is 33 months. The research results provide technical support for the water treatment process upgrade of the thermal power plant.

Keywords: Coagulation and full-membrane technique; Municipal reclaimed water; Environmentally friendly; Response surface optimization; Boiler feedwater

1. Introduction

"Seventeen sustainable development goals" and "affordable and clean energy" are pointed out in "2030 Agenda for Sustainable Development (United Nations, January 1st, 2016)" [1]. China is facing depletion in freshwater resources. The water resources per capita recorded are merely 2,300 tons and it is only 25% of the world average [2]. China is one of the countries with minimum freshwater resources per capita in the world. At the same time, China is the biggest

* Corresponding author.

consumer of fresh water in the world, and the demand for freshwater is drastically increased with economic prosperity. The northern China is highly populated and industrial growth has ascended. This area is also producing higher yield in agriculture field that results in an aggravating shortage of freshwater [3].

Now, with the development of the urbanization process in China. Population in urban areas of China is increasing exponentially. The handling capacity of urban wastewater treatment in cities and towns has been increased since after the development of the urbanization process. In order to control water pollution, a large number of urban wastewater treatment plants have been erected. At present, the rate of urban wastewater treatment in China has reached 93.44%. The development of wastewater treatment plants has increased the total production of municipal reclaimed water after secondary treatment. Meanwhile, the use rate of municipal reclaimed water is only 45% [4]. Wen et al. [5] pointed out that the residents of urban areas do not like to use recycled water and the degree of dislike of using treated water by urban area residents is directly linked with their political ideology. But industrial reuse of municipal reclaimed water remains relatively unaffected by the community's trust in recycled water. Water Pollution Prevention Action Plan has been published by the State Council of China on April 16th, 2015. In this plan, it is emphasized that industries should give priority towards to the utilization of recycled water during production, and industries should be able to use the municipal reclaimed water partly if it cannot use completely, and permission of fresh-water inflow is prohibited for industries like steelworks, thermal power plants, chemical industries, pulp and paper making industries, printing and dyeing, textile printing, and other projects alike [6].

China has high energy demand, and it is rich in coal reserves but at the same time, it has a lower amount of oil and natural gas reserves [7]. The limitations of wind energy, hydroelectric energy, solar energy, and nuclear energy results in the booming of coal-fired energy generation companies. According to statistics, the northern region of China contains 93.1% of the national coal reserves but in this region has only 19% of the total volume of national water resources [8,9]. The circulating makeup water needs plenty of treated water in the coal-fired wet-cooled power plant. Thermal power plants are different than other normal power plants. The huge evaporation takes place in cooling circulating water, while a large amount of steam is extracted from the steam extraction pipe of steam turbine medium pressure cylinder for residents heating purposes. The environmental protection policies have become more strict results in making the municipal reclaimed water as an essential source of thermal power plant [10].

The utilization of municipal reclaimed water in thermal power plants as their main water source. This is not only an economical process but also can further improve the local environment ecologically. The municipal reclaimed water has higher turbidity, hardness, and total suspended solids (TSS). It is rich in organic substances and it contains compounds of nitrogen and phosphorous [11]. Nitrogen and phosphorus are the essential nutrients for microbial growth. Suspended solids (SS), higher turbidity, and hardness can cause scaling in the pipelines of the thermal equipment while chloride ions cause corrosion in carbon steel and stainless-steel pipelines. For pre-treatment, it is difficult to remove nitrogen, hardness, and chemical oxygen demand (COD) from water by traditional coagulation and sedimentation processes completely. For the demineralized water treatment, the ion-exchange regeneration process produces a large amount of acid–base wastewater. The comparison of the traditional water treatment process and coagulation full-membrane process in thermal power plant show that the coagulation and the full-membrane process has an obvious advantage over the traditional water treatment process. The coagulation and the full-membrane process has high integrity, operation, and maintenance convenient as compared to traditional coagulation and sedimentation processes. In order to provide the reference for the designers and researchers through an engineering example in northern China, a comprehensive analysis report on coagulation-membrane process and applications of coagulation and the full-membrane process is also discussed in this paper.

2. Engineering design

2.1. Geological and climatic characteristics

The project is located in Baoding city, Hebei province, China, as shown in Fig. 1. Baoding city is a semi-arid and semi-humid region that belongs to the eastern monsoon region that has a continental monsoon climate and mildly warm temperature zone. The annual average temperature has recorded is 12.6°C. The maximum and minimum temperature is 42.2°C and –23.4°C, respectively. The average annual rainfall has recorded is 551.4 mm and maximum rainfall is recorded in July–August, which is more than 60% of the total annual rainfall. The maximum amount of freshwater used by urban residents is obtained from underground water resources as the surface water resources depletion and water replenishment from south to north in Hebei province is also limited. The freshwater resources are also alarming because the water resources are not sustainable in Hebei province, China [12,13].

2.2. Quality and quantity of water

The power plant uses municipal reclaimed water treated by the two wastewater treatment plants as its main water source. The water from south-to-north water transfer project is used as an emergency standby water source. The plant uses municipal tap water as its domestic water source. The industrial firefighting water of the power plant is treated by a coagulation system. The water produced by the municipal reclaimed water pre-treatment system is 1,600 t/h. The quality of municipal reclaimed water from two wastewater treatment plants and surface water flow from south-to-north water transfer project are shown in Table 1.

It can be seen from Table 1 that the salinity, total hardness, total alkalinity, total number of bacteria, ammonia nitrogen, total phosphorus, COD, and biochemical oxygen demand (BOD_5) of two wastewater-treatment plants treated water are higher than the water flow from south-to-north water transfer project. But the appearance, odor, and turbidity are basically the same.

Fig. 1. Research sites.

Table 1
Water quality of municipal reclaimed water and the south-to-north water transfer project water

Test items		Detection result					
		Lugang waste-treatment plant treated water		Yuquan waste-treatment plant treated water		Water from south-to-north water transfer project	
		mg/L	mmol/L	mg/L	mmol/L	mg/L	mmol/L
Cation	Na^+	91.90	4.00	77.70	3.38	6.33	0.28
	K^+	14.30	0.37	11.86	0.30	3.52	0.09
	Ca^{2+}	87.57	4.37	75.55	3.77	33.87	1.69
	Mg-ions	38.88	3.20	32.56	2.68	10.69	0.88
	Total iron	0.052	0.0028	0.048	0.0026	–	–
	Total copper	0.42	0.013	0.30	0.0094	0.42	0.013
	Total aluminum	0.13	0.014	0.083	0.0092	0.095	0.011
	Sr^{2+}	4.52	0.10	4.14	0.094	4.07	0.093
	Sum of cations per unit charge	12.07		10.25		3.06	
Anion	OH^-	0.00	0.00	0.00	0.00	0.00	0.00
	$1/2CO_3^{2-}$	0.00	0.00	0.00	0.00	0.00	0.00
	HCO^{3-}	272.76	4.47	275.81	4.52	119.60	1.96
	Cl^-	139.40	3.93	141.00	3.98	9.00	0.25
	$1/2SO_4^{2-}$	130.23	2.71	25.52	0.53	35.93	0.75
	NO^{3-}	58.03	0.94	61.44	0.99	2.17	0.035
	NO^{2-}	0.14	0.0030	0.18	0.0039	–	–
	PO_4^{3-}	1.04	0.033	6.07	0.19	0.00081	–
	Sum of anions per unit charge	12.09		10.21		3.00	
Other items	Appearance	Transparent		Transparent		Transparent	
	Smell	Odorless		Odorless		Odorless	
	Turbidity	2.95	NTU	1.25	NTU	3.52	NTU
	Total hardness	7.57	mmol/L	6.45	mmol/L	2.57	mmol/L
	Total alkalinity	4.47	mmol/L	4.52	mmol/L	1.76	mmol/L
	Bacterial numbers	410	units/mL	130	units/mL	38	units/mL
	Ammonia nitrogen	0.74	mg/L	0.57	mg/L	0.060	mg/L
	Total phosphorus	1.80	mg/L	6.19	mg/L	0.0025	mg/L
	COD	17	mg/L	21	mg/L	2	mg/L
	BOD_5	4.50	mg/L	4.85	mg/L	0.21	mg/L

Due to the high concentration of Na^+, Cl^-, and SO_4^{2-} in the municipal reclaimed water, in order to prevent the growth of bacteria, adding NaClO to the system and maintaining a certain concentration will help prevent bacterial contamination in the system. As the increase of the NaOCl dosage, the pH, chloride concentration, and Larson index increased correspondingly due to the hydrolysis reaction of NaOCl. On the other hand, the hydrolysis of NaOCl increased pH favored the conversion of bicarbonate into carbonate and yielded precipitation. NaOCl has multiple effects on corrosion and scaling. Like liquid chlorine, NaOCl can accept electrons from iron substrate or oxidize ferrous ions to ferric oxide or hydroxide in bulk water, which enhances corrosion. Unlike liquid chlorine, the alkaline NaOCl solution favors $CaCO_3$ formation and deposition, especially in high alkalinity and hardness water, and present different effects on corrosion [14,15]. At the same time, due to the increase of Cl^- ion concentration, the risk of corrosion to basic structures such as concrete, stainless steel, and carbon steel will also increase correspondingly, especially the corrosion relationship with a high concentration of SO_4^{2-} on concrete should be paid more attention [16,17]. Moreover, excessive sodium ions can be removed by reverse osmosis and EDI systems, so that the final effluent reaches the qualified standard.

2.3. Municipal reclaimed water pre-treatment system

Municipal reclaimed water pre-treatment system is designed to meet the water demand and zero discharge of wastewater in the thermal power plant. This system is established to protect the environment. The designed capacity of the municipal recycled water advanced treatment system is 2 × 800 t/h. The water treatment dosing system contains a bactericide adding unit, calcium hydroxide adding unit, coagulant adding unit, flocculant adding unit, and sulfuric acid adding unit. Hardness, ammonia–nitrogen, total phosphorus, turbidity, COD, and BOD_5 are partly removed from recycled water through a coagulation pre-treatment system by adjusting the pH of water [18–20]. This can reduce the scaling tendency and operational difficulties of the full-membrane processing system. In the coagulation water pre-treatment system, sulfuric acid (H_2SO_4) is added to maintain the pH value so that water remains stable neutral pH. The process flow diagram indicating water balance under full-load of the unit. The water demand in summer and winter is out and in the brackets is shown in Fig. 2, respectively.

2.4. Full-membrane water treatment system

In order to meet the requirements of water quality of supercritical units and reduce the discharge of acid and alkali wastewater regenerated, full-membrane water treatment system is designed after the coagulation water pre-treatment system.

Membrane flux is decreased in winter because the temperature of raw water is low which disturbs the standard flow of ultra-filtration (UF) and reverse-osmosis (RO) system [21]. Two mixed steam heaters of capacity 2 × 300 t/h are designed at the inlet of the raw water tank. The auxiliary steam from auxiliary steam header to heat the treated water from municipal reclaimed water pre-treatment system. The heater is designed to keep the inlet water temperature of the full membrane water treatment system nearby 25°C.

Three dual media filters (DMF) with a flow capacity of 300 t/h are installed before the UF unit to remove the large particulate matter and suspended particles from raw water. Each DMF is filled with 6.5 m^3 of quartz sand and 3.5 m^3 of anthracite. Quartz sand is soaked in the acid solution for 24 h before filling in the DMF. After filling the quartz sand and anthracite into DMF, it is backflushed for an adequate time. The UF system uses PVDF external pressure hollow fiber membranes for the removal of contaminants in water and removes large molecules such as proteins, colloids, suspensions, macro-molecular organics, and microorganisms of size 0.001 to 0.1 μm. There are three UF units installed and the flow capacity of each UF unit is 160 t/h. There are 20 membrane elements installed in each UF unit.

The RO membrane can almost remove dissolved salts and all micro molecule organic matter from water. Salt rejection rate is usually above 96% which means it can effectively remove micro molecule organic substances, heavy metals, sulfates, phosphates, and hardness in water. The RO system contains spiral coil structure membrane components. The whole series contains three first stage reverse-osmosis (RO_1) series and two second-stage reverse-osmosis (RO_2) series. The flow capacity of RO_1 is 144 t/h and RO_2 is

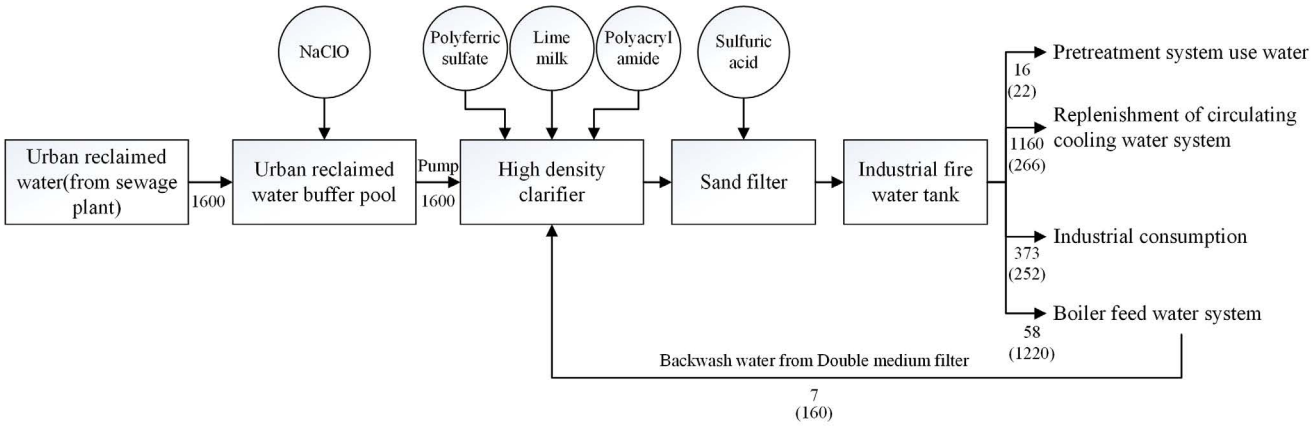

Fig. 2. Water balance of the coagulation water pre-treatment system.

122 t/h. There are 36 reverse-osmosis elements installed in each RO_1 series and each RO_2 series install 17.

To meet the stringent specification of the power plant, cation conductivity (CC), and silica (SiO_2) of boiler feedwater must be maintained at CC ≤ 0.10 μS/cm and SiO_2 ≤ 10 μg/L. Water produced from RO systems could not meet the water quality requirements of supercritical units. This is the reason that continuous electro deionization (CEDI) systems are installed after the RO systems. There are three fundamental phenomena that take place in a CEDI systems device. Water purification is treated by ion exchange between the ions present in inlet water and functional groups attached with ion-exchange resin when a direct current is applied to migrate the ions in CEDI systems. The electrolyzed water helps regeneration of ion-exchange resin in CEDI systems device. The CEDI systems are environmentally friendly devices because they never produce waste acid and alkali.

The process flow diagram indicating the water balance of the full-membrane water treatment system. The water demand in summer and winter is out and in the brackets is shown in Fig. 3, respectively.

3. Coagulation and full-membrane treatment system operation

The test operation of coagulation and full-membrane treatment of municipal reclaimed water started in July 2018. In summer, the temperature of northern China has increased and the temperature drop is very small between day and night. Therefore, the temperature of the water changes slightly. But the quality of municipal reclaimed water changes significantly with rainfall.

3.1. Optimal operation of municipal reclaimed water treatment system

The municipal reclaimed water from the wastewater treatment plant is stored in recycled water buffer pools. The NaClO is added to the buffer pool and used as a disinfectant in the municipal reclaimed water pre-treatment system. There are many bactericide categories available but preference has been given to sodium hypochlorite (NaClO) as N.F. Gray described in his book "Microbiology of Waterborne Diseases (2nd edition)" that NaClO is a very effective biocide that also has residual disinfection effect and controls biofilm production [22].

Water quality is greatly influenced by rainfall and the introduction of CO_2 from the air, so an increase in carbonic acid and lime added results in an increase in $CaCO_3$ precipitates. The colloidal particles are entangled by calcium carbonate crystals in the same way as aluminum and iron flocs. When lime is introduced in water then pH will rise and water can become chemically unstable so there is a need to lower the pH value at optimum conditions [23]. The coagulant is added then all metal salts hydrolyze immediately and form cation species at an isoelectric point which then will be adsorbed by negatively charged particles so the surface charge is reduced and micro flocs are produced [24]. The settling velocity of micro flocs is lower and they remain dispersed in the clarifier zone so polymeric flocculant anionic/non-ionic is dosed to increase the adhesive forces between micro flocs and larger and denser flocs. They are formed with high settling velocities so that removal of large flocs is facilitated in sequent sedimentation, flotation, and filtration stages [25]. Since PAM will pollute the subsequent membrane treatment equipment and it is not allowed in the industrial standard, the coagulant of PAM is not added in this test [26]. Since macromolecule long-chain flocculants have a better flocculation effect [24,27], in order to achieve a better flocculation effect and save cost, it is necessary to use macromolecule flocculants. Cheng [29] pointed out that polymerized ferrous sulfate (PFS) is a polyelectrolyte compound with molecular formula of $[Fe_2(OH)n(SO^4)_{3-n/2}]_m$ ($n < 2$, $m > 10$). It contains a range of pre-formed hydrolysis species, $[Fe(OH)_x]^{(3-x)+}$ and $[Fe_m(OH)_x]_n^{(3m-x)n+}$ of iron(III), including $[Fe_2(OH)_3]^{3+}$, $[Fe_2(OH)_3]_2^{6+}$, and $[Fe_8(OH)_{20}]^{4+}$ etc. Generally, the polymers carry a high cationic charge. Their surface activity and charge neutralizing capacity make them more competitive than the conventional coagulants [28,29]. It is difficult to increase the removal efficiency of organic and suspended loads by only use PFS at lower pH so calcium hydroxide is added in the coagulation process to increase the removal of such impurities by increase the pH value. Ismail et al. [19] have performed a series of tests and removal efficiency of coagulants such as ferric sulfate, ferrous sulfate, and combination of ferrous sulfate and lime combined is determined based on TSS, BOD, $(PO_4)^{3-}$, and COD removal percentage during coagulation and clarification process [19]. The results show that when the combination of ferrous

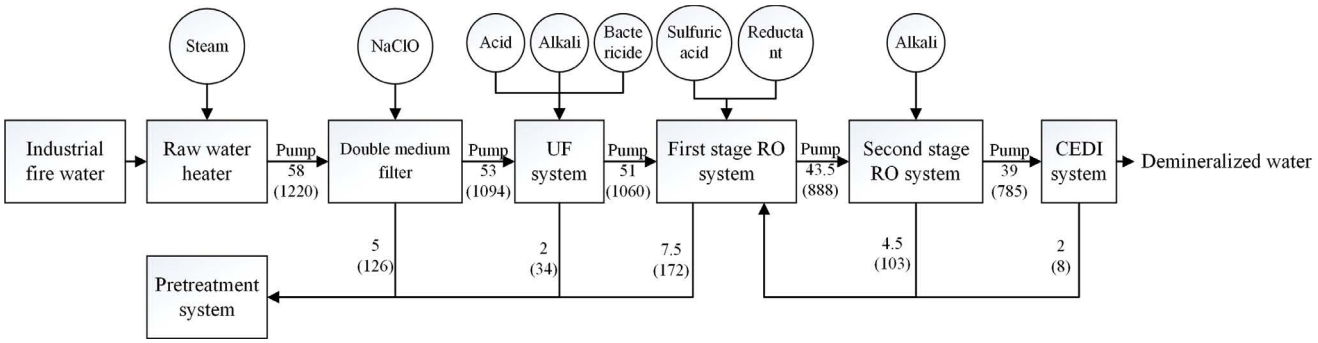

Fig. 3. Water balance of full-membrane water treatment system.

sulfate and lime combined is used instead of ferrous sulfate alone then the removal rate of TSS, BOD, $(PO_4)^{3-}$, and COD is increased by 4%, 2%, 4%, and 4%, respectively [30]. The maximum flow rate in the clarification zone was not increased above 2.0 mm/s. The pH at the outlet of the mixing zone is neutralized by adding H_2SO_4. In the clarification zone of the high-density clarifier, the large particulate matter is removed by sedimentation while the small particulate matter is removed by trapping action of particulate matter. The residual particulate matter is further removed by the sand filter with an adsorption and bridging process. The filtered water is stored in an industrial firefighting tank.

Because there are many concrete structural foundations, carbon steel pipes, and stainless steel pipes in the system, the water quality in the test is not allowed to be acidic strictly [31–33]. The municipal reclaimed water in the urban reclaimed water buffer pool is used as the test water sample. The pH of the municipal reclaimed water is 7.45 and the turbidity is 12.62. Adjust the pH by adding lime, stir for 2 min at 400 rpm, and for 2 min at 60 rpm, observe the sedimentation speed of flocs in the water sample at pH 8, 9, 10, 11, and 12, respectively. The turbidity of the sample supernatant liquor was measured after 15 min of sedimentation as shown in Fig. 4.

It can be seen from Fig. 4 that by adding the lime solution to the municipal reclaimed water, the sedimentation speed of flocs, and the turbidity of the sample supernatant liquor decrease with the increase of pH. When the pH is over 10, the sedimentation speed and the turbidity of the sample supernatant liquor change slowly. When pH is over 12, it is basically stable. According to the results of small-scale tests and considering the economy of industrial equipment, the pH value of about 10 is the most reasonable in the actual application process.

Design Expert 11.0.4 software (Stat-Ease Inc., Minneapolis, US) was utilized for design, mathematical modeling, and optimization. The variables (independent factors) used in this study were: polyferric sulfate (PFS) dosage (X_1), NaClO dosage (X_2), and stirring rate in flocculant area (X_3). Turbidity, COD, and NH_3–N removal rate were considered as the dependent factors (response) (Y_1, Y_2, and Y_3, respectively). Performance of the process was evaluated by analyzing the turbidity, COD, and NH_3–N removal rate.

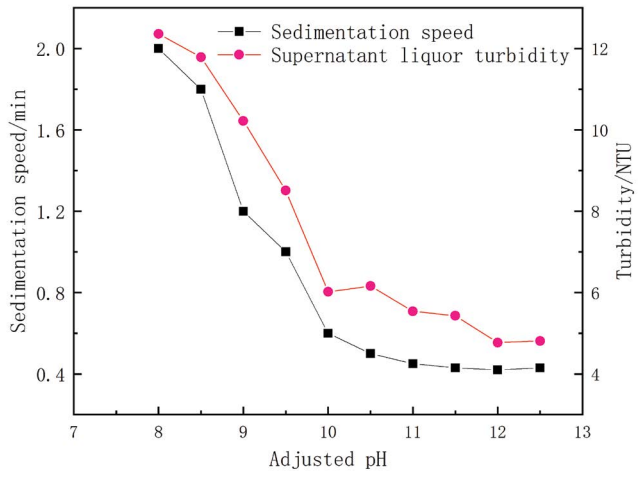

Fig. 4. Sedimentation speed of flocs and the turbidity of the sample supernatant liquor in small-scale tests.

At the same time, temperature (20°C), pH of flocculant area adjusted by adding calcium hydroxide (10.1), rate of inflow (800 t/h), and pH of effluent adjusted by adding H_2SO_4 (6.5) were kept constant to reduce the number of factors and to simplify the test design. According to Box–Behnken response surface analysis method, turbidity removal rate Y_1, COD removal rate Y_2, and ammonia NH_3–N removal rate Y_3 were used as response values to design three-factor and three-level tests. The test design and results are shown in Table 2. Multiple regression fitting was performed on the test data in the table, and the regression analysis results of each response value were shown in Table 3. Meanwhile, the quadratic regression models of turbidity removal rate Y_1, COD removal rate Y_2, and ammonia NH_3–N removal rate Y_3 were obtained as Eqs. (1)–(3).

Eqs. (1)–(3) present the models for percentage turbidity, COD, and NH_3–N removal rate:

$$Y_1 = 84.66 + 2.97X_1 - 0.45X_2 - 0.125X_3 + 0.675X_1X_2 - 1.28X_1X_3 - 0.225X_2X_3 - 8.19X_1^2 + 1.16X_2^2 - 5.44X_3^2 \quad (1)$$

$$Y_2 = 87.78 + 1.65X_1 + 2.85X_2 - 1.18X_3 - 0.15X_1X_2 + 0.55X_1X_3 + X_2X_3 - 2.62X_1^2 - 3.82X_2^2 - 1.71X_3^2 \quad (2)$$

$$Y_3 = 85.48 + 1.58X_1 + 4.43X_2 + 0.375X_3 + 0.175X_1X_2 + 0.225X_1X_3 - 0.375X_2X_3 - 3.5X_1^2 + 0.1975X_2^2 - 1.1X_3^2 \quad (3)$$

The results of variance analysis and significance test for the quadratic regression equation are shown in Tables 4–6. The model variance analysis and significance test are important methods to measure the rationality of model design and prediction ability. The *F*-value of the model is 118.87, 355.26, and 30.1 (Y_1, Y_2, and Y_3, respectively). All of the *p*-value of model is <0.0001 (Y_1, Y_2, and Y_3). The lack of fit of the model is 0.3907, 0.2534, and 0.6955 (Y_1, Y_2, and Y_3, respectively). It shows that all three models are significant, reliable, and accurate.

As shown in Table 7, the signal to noise ratio of the three models is 33.5381, 55.5754, and 17.6281 (Y_1, Y_2, and Y_3, respectively), which are all greater than 4. The data indicating that the three models all provide an adequate signal to respond to the design and has a high degree of authenticity. The R^2 coefficients of the three model are 0.9935, 0.9978, and 0.9748 (Y_1, Y_2, and Y_3, respectively), which are all greater than 0.8 that indicating the good fitting degree of the three model and the test error is little. The adjusted R^2 coefficient

Table 2
Independent variables and their levels for the BBD

Symbol	Factor	Levels		
		–1	0	1
X_1	PFS dosage, mg/L	25	30	35
X_2	NaClO dosage, mg/L	3	4	5
X_3	Stirring rate, rpm	200	300	400

Table 3
Experimental matrix design

Std	Run	PFS dosage (mg/L)	NaClO dosage (mg/L)	Stirring rate (rpm)	Turbidity removal rate (%)	COD removal rate (%)	NH_3–N removal rate (%)
11	1	30	3	400	80.3	77.1	80.8
4	2	35	5	300	80.4	85.8	87.9
15	3	30	4	300	84.9	88.1	86.5
1	4	25	3	300	76.2	76.6	76.8
16	5	30	4	300	85.2	87.6	86.6
9	6	30	3	200	80.7	81.8	79.5
8	7	35	4	400	73	84.6	83.6
10	8	30	5	200	80.9	85.4	89.1
2	9	35	3	300	80.6	80.3	78.7
3	10	25	5	300	73.3	82.7	85.3
6	11	35	4	200	75.2	85.5	82.2
5	12	25	4	200	66.5	83.4	78.6
12	13	30	5	400	79.6	84.7	88.9
14	14	30	4	300	84.3	87.9	85.3
17	15	30	4	300	85.2	87.7	84.8
7	16	25	4	400	69.4	80.3	79.1
13	17	30	4	300	83.7	87.6	84.2

Table 4
Analysis of variance for response surface quadratic model terms for turbidity removal

Source	Sum of squares	DF	Mean square	*F*-value	*p*-value	Remark
Model	510.02	9	56.67	118.87	<0.0001	Significant
X_1	14.11	1	14.11	29.59	0.0010	Significant
X_2	7.11	1	7.11	14.92	0.0062	Significant
X_3	0.0267	1	0.0267	0.0559	0.8198	Not significant
X_1X_2	1.82	1	1.82	3.82	0.0915	Not significant
X_1X_3	6.50	1	6.50	13.64	0.0077	Significant
X_2X_3	0.2025	1	0.2025	0.4248	0.5354	Not significant
X_1^2	282.60	1	282.60	592.80	<0.0001	Significant
X_2^2	5.64	1	5.64	11.83	0.0108	Significant
X_3^2	124.72	1	124.72	261.62	<0.0001	Significant
Residual	3.34	7	0.4767			
Lack of fit	1.64	3	0.5483	1.30	0.3907	Not significant
Pure error	1.69	4	0.4230			
Cor. total	513.36	16				

of the model showed that the three models could explain the variation of response values of 98.51%, 99.50%, and 94.24% (Y_1, Y_2, and Y_3, respectively), and only 1.49%, 0.50%, and 5.76% of the total variation could not be explained by this model. The three models show good regression. In conclusion, this model can be used to analyze and predict the removal of turbidity, COD, and ammonia nitrogen in municipal reclaimed water treatment system.

The response surfaces of each interaction factor to turbidity, COD, and NH_3–N removal efficiencies are shown in Figs. 5–7. The influence of the interaction between any two factors on the response value can be analyzed and evaluated to determine the optimal factor level. The surface slope can reflect the influence of factors on the response value. The steeper the slope, the greater influence of factors on the response value. The strength of the interaction between factors is reflected by the contour shape.

As shown in Fig. 5, the interaction between the PFS dosage and the stirring rate is extremely significant, while the interaction between the PFS dosage and the NaClO dosage, the NaClO dosage, and the stirring rate is not significant. It is proving that the PFS dosage has the most significant influence on turbidity removal efficiency. As shown in Fig. 5a, the influence of NaClO on the turbidity is relatively

Table 5
Analysis of variance for response surface quadratic model terms for COD removal

Source	Sum of squares	DF	Mean square	*F*-value	*p*-value	Remark
Model	216.05	9	24.01	355.26	<0.0001	Significant
X_1	21.78	1	21.78	322.33	<0.0001	Significant
X_2	64.98	1	64.98	961.65	<0.0001	Significant
X_3	11.05	1	11.05	163.46	<0.0001	Significant
X_1X_2	0.0900	1	0.0900	1.33	0.2863	Not significant
X_1X_3	1.21	1	1.21	17.91	0.0039	Significant
X_2X_3	4.00	1	4.00	59.20	0.0001	Significant
X_1^2	28.79	1	28.79	426.11	<0.0001	Significant
X_2^2	61.28	1	61.28	906.91	<0.0001	Significant
X_3^2	12.38	1	12.38	183.27	<0.0001	Significant
Residual	0.4730	7	0.0676			
Lack of fit	0.2850	3	0.0950	2.02	0.2534	Not significant
Pure error	0.1880	4	0.0470			
Cor. total	216.52	16				

Table 6
Analysis of variance for response surface quadratic model terms for NH_3–N removal

Source	Sum of squares	DF	Mean square	*F*-value	*p*-value	Remark
Model	237.16	9	26.35	30.10	<0.0001	Significant
X_1	19.85	1	19.85	22.67	0.0021	Significant
X_2	156.65	1	156.65	178.94	<0.0001	Significant
X_3	1.13	1	1.13	1.29	0.2943	Not significant
X_1X_2	0.1225	1	0.1225	0.1399	0.7194	Not significant
X_1X_3	0.2025	1	0.2025	0.2313	0.6452	Not significant
X_2X_3	0.5625	1	0.5625	0.6425	0.4491	Not significant
X_1^2	51.65	1	51.65	59.00	0.0001	Significant
X_2^2	0.1642	1	0.1642	0.1876	0.6779	Not significant
X_3^2	5.12	1	5.12	5.85	0.0462	Significant
Residual	6.13	7	0.8754			
Lack of fit	1.70	3	0.5667	0.5119	0.6955	Not significant
Pure error	4.43	4	1.11			
Cor. total	243.29	16				

Table 7
Quadratic model ANOVA results for turbidity, COD, and NH_3–N removals

Variable	Turbidity removal	COD removal	NH_3–N removal
Standard deviation	0.6904	0.2599	0.9356
Mean	78.79	83.95	83.41
R^2	0.9935	0.9978	0.9748
R^2 adjusted	0.9851	0.9950	0.9424
R^2 predicted	0.9436	0.9776	0.8598
Coefficient of variance (%)	0.8763	0.3097	1.12
Adequate precision	33.5381	55.5754	17.6281

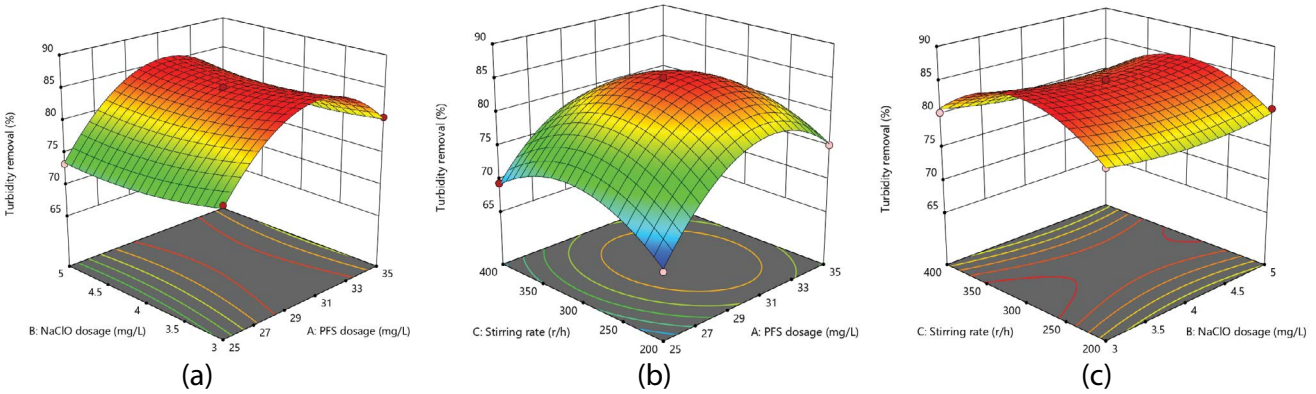

Fig. 5. Response surface diagram of the influence of each interaction factor on turbidity removal rate: (a) PFS dosage and NaClO dosage, (b) PFS dosage and stirring rate, and (c) NaClO dosage and stirring rate.

small with the increase of the dosage. If the dosage of PFS is insufficient, effective charge neutralization of suspended matter in water in water cannot be carried out at the designed flow rate. If the dosage of PFS is too high, the suspended matter in the water will be positively charged, and the removal rate of turbidity will be reduced. The hydrolysis of NaClO was beneficial to the coagulation effect of PFS. At the same time, the hydrolysis of NaClO at different dosages has a lower effect on the removal of turbidity with PFS. As shown in Fig. 5b, the dosage of PFS and the stirring rate show a good interaction. With the proper dosage of PFS dosage and the stirring rate, the chance of particle collision can be increased, and the removal of turbidity can be enhanced. As shown in Fig. 5c, too fast a speed rate will cause the turbidity of the effluent to decrease. In the selected experimental range, when the PFS dosage was 31.02 mg/L, the NaClO dosage was 4.92 mg/L, the stirring rate was 315.42 rpm, and the turbidity removal efficiency is the maximum 85.405%.

As shown in Fig. 6, the interaction between three influence factors all is extremely significant. If the PFS dosage and the stirring rate are insufficient or too high, the coagulation effect will decrease. Thereby affecting the removal of organic matter, resulting in a decrease in the COD removal rate. The NaClO is a strong oxidant that can oxidize a part of the organic matter, but excessive NaClO will destabilize the slime in the water. At the same time, as the content of chloride ions increases added by the NaClO, the impact of chloride ions on COD measurement is also causes a decrease in COD removal rate. In the selected experimental range, when the PFS dosage was 31.56 mg/L, the NaClO dosage was 4.67 mg/L, the stirring rate was 266.55 rpm, and the COD removal rate is the maximum 88.14%.

As shown in Fig. 7, the effect of NaClO on the removal of NH_3–N in water is relatively significant. The content of available chlorine in the water increases with the NaClO dosage, which has a significant effect on the removal of NH_3–N. However, the PFS dosage and the stirring rate have a maximum value for the removal of NH_3–N, and the removal effect is not as good as that of the NaClO dosage. In the selected experimental range, when the PFS dosage was 29.65 mg/L, the NaClO dosage was 4.89 mg/L, the stirring rate was 336.00 rpm, and the NH_3–N removal rate is the maximum 89.29%.

The combination of optimal conditions obtained by response surface and combine with the actual situation. In conclusion, the response surface analysis showed that the optimal conditions for the removal rate of turbidity, COD, and NH_3–N in municipal reclaimed water treatment system were as follows: the PFS dosage is 30 mg/L, the NaClO dosage was 4.5 mg/L, the stirring rate is 300 rpm. Under these conditions, COD and NH_3–N removal rate is 84.72%, 88.25%, and 87.74%, respectively. The operation data of the municipal reclaimed water treatment system from August to October is shown in Fig. 8. After the coagulation system, the main indexes of the municipal reclaimed water quality after pre-treatment have been effectively achieved. The effect of inlet water temperature on the coagulation process should be paid attention during operation.

3.2. Operation effect of the full-membrane water treatment system

3.2.1. DMF and UF system

The DMF are installed to remove the suspended particles in water and protect the UF membranes. Ncube et al. [34] pointed out that multimedia filters are more efficient than single media filter. It was clear from his research that for both single and multimedia filters the TSS removal rate was increased with the media bed depth, but at the same time, filter head loss is prominent with high bed depth and filtration time. It was evident that if more solids were retained then filter head loss was increased for all types of media filters [35]. The DMF is backwashed once a week to restore its performance. The UF system has a production cycle of 40 min and it is scrubbed with air and flushed with water after every production cycle. After 12 production cycles is an acid cleaning process. After another 12 production cycles, an alkali and bactericide cleaning process perform. The UF water recovery rate was controlled at 92%. Regular maintenance sterilization in operation to prevent the growth of bacteria in the UF system. In order to fully utilize the water resources, wastewater from DMF, and UF is recycled to municipal recycled water advanced treatment system. The operating data of DMF and UF system from August to October is shown in Fig. 9. The turbidity of outlet

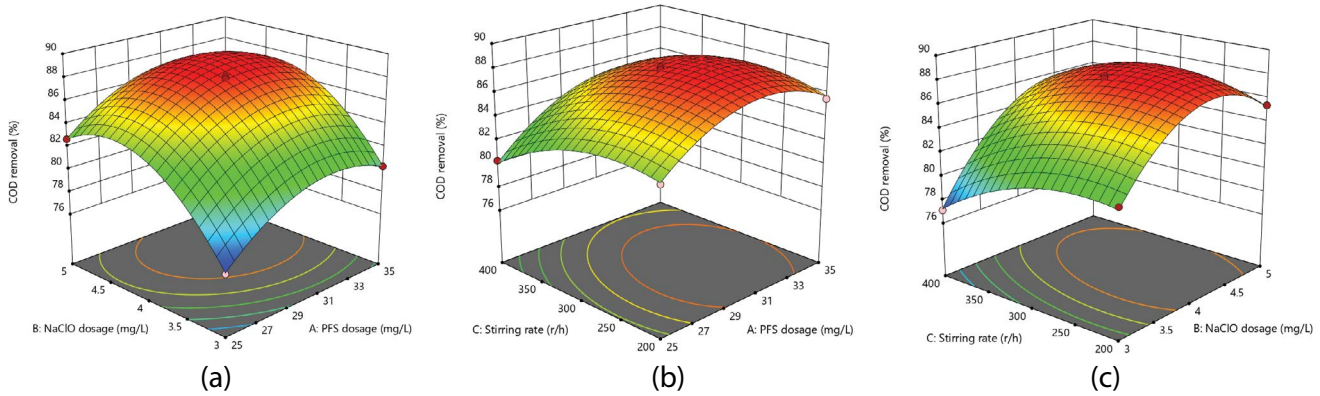

Fig. 6. Response surface diagram of the influence of each interaction factor on COD removal rate: (a) PFS dosage and NaClO dosage, (b) PFS dosage and stirring rate, and (c) NaClO dosage and stirring rate.

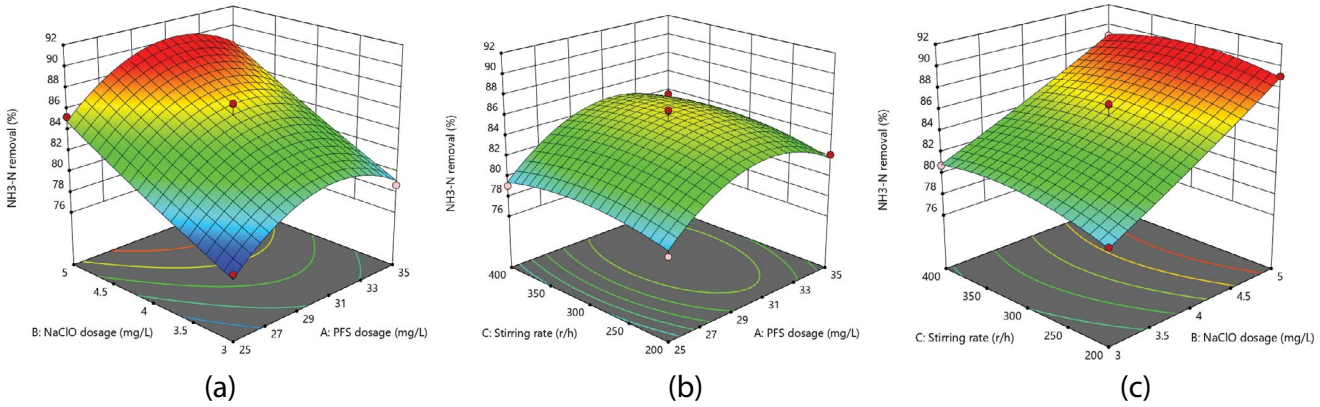

Fig. 7. Response surface diagram of the influence of each interaction factor on NH_3–N removal rate: (a) PFS dosage and NaClO dosage, (b) PFS dosage and stirring rate, and (c) NaClO dosage and stirring rate.

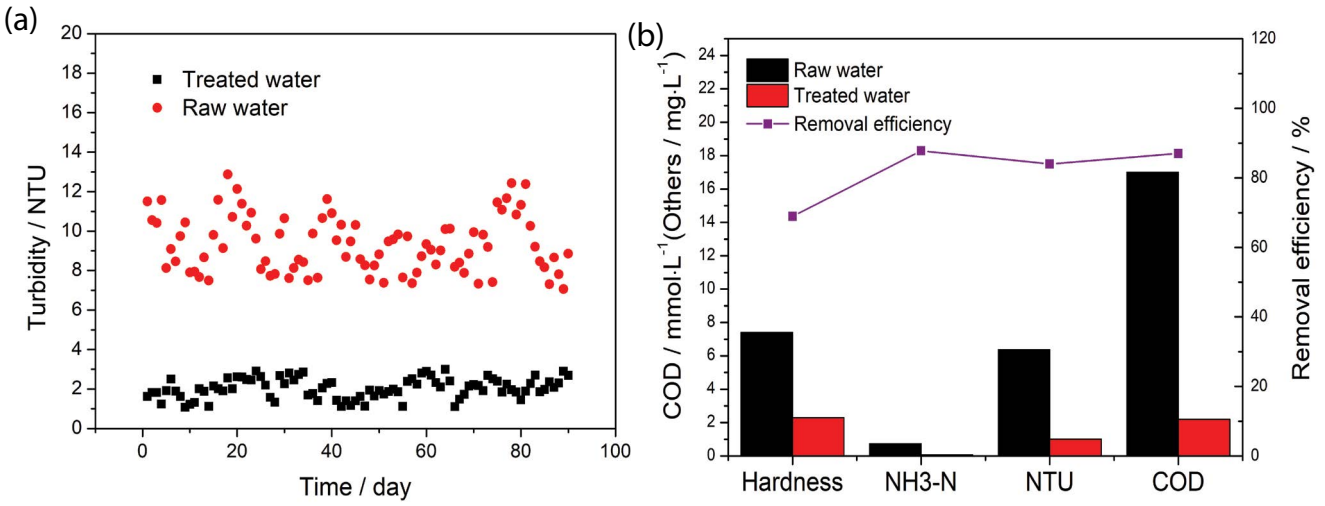

Fig. 8. Purification effect of municipal reclaimed water treatment system on water quality: (a) turbidity of inlet and outlet water and (b) hardness, NH_3–N, NTU, COD concentration, and removal efficiency after post-optimality.

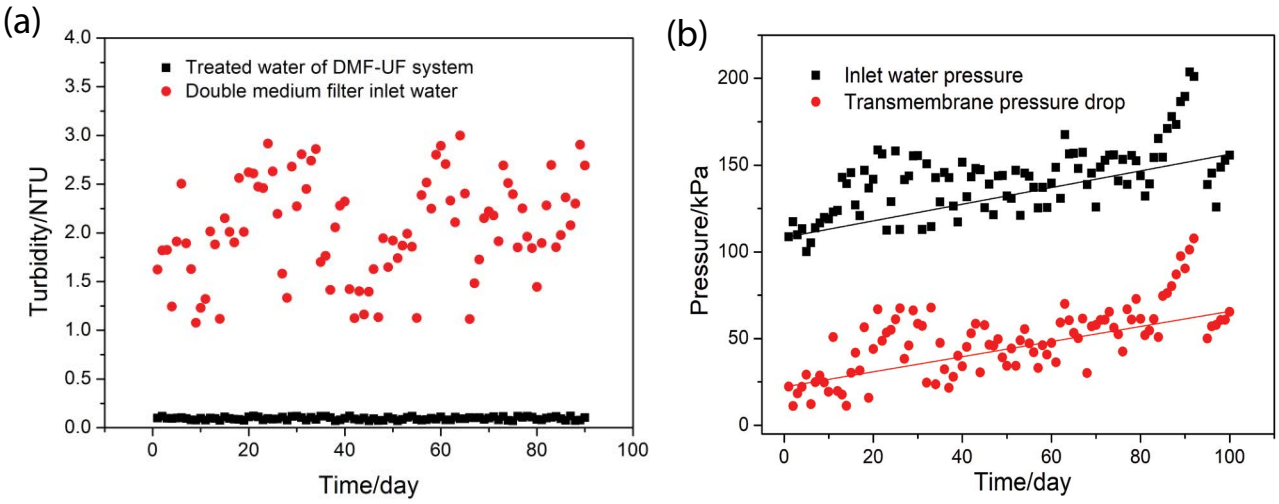

Fig. 9. DMF and UF system operation (a) DMF-UF effectively decrease the NTU and (b) TMP increased with inlet water pressure.

water reaches below 0.1 NTU when processed through DMF and UF systems. The inlet pressure (IP) and trans-membrane pressure drop (TMP) are increased to some extent with the passage of time so should be paid attention to UF operation. As the pore size of the UF is not enough to trap ammonia nitrogen and small organic matter, the removal efficiency of COD and ammonia nitrogen is only 4.7% and 10.3%. The operating parameters play an important role in membrane separation processes [36]. Wu et al. [37] found that if the operating pressure is increased then retention of contaminants will be decreased. So, it is clear that knowing the effects of operating parameters on membrane separation processes the effect of fouling could be decreased effectively. The feedwater temperature was increased then permeate flux was increased and when transmembrane pressure was increased then permeate flux increased also and then a decreasing trend was witnessed [38].

When the TMP drop reaches the upper limit 100 kPa then the corresponding UF membrane needs to be chemically cleaned. Chemical cleaning is performed to prevent UF membrane from damage, restore the performance, and increase the service life of UF system. During the UF system test-operation, the transmembrane pressure drops increase fast so that the system cannot run stably and chronically. We analyze the system operation state and the contaminant in system back-wash water. We find there is a phenomenon that the PFS coagulant pollutes on the membrane surface. After decreasing the dosage of PFS and chemical cleaning the UF system off-line, the UF system returns to normal running.

3.2.2. Operation effect of RO system

Reverse osmosis (RO) and nanofiltration (NF) techniques are extensively used in water treatment system because of their high performance and low operation cost. The membranes of RO and NF are TFC type membranes made of three layers [39]. The top layer is made of polyamide which is the basic concern and performance of RO is strongly dependant on the integrity of polyamide layer [40]. Residual chlorine in water strongly affects the performance of the polyamide layer of RO. The performance decay was witnessed when oxidizing species is subjected to polyamide, life span would be decreased, and operation costs will be higher. The reducing agent is being added at the inlet of RO device to mitigate the effect of residual oxidizing chlorine on RO membrane. Verbeke et al. [41] further investigated the effect of temperature on the presence of chlorine as HOCl. He proposed that with the increase in temperature amount of chlorine present in water as HOCl was lower pH is an important variable that has an effect on chlorine presence in feed water. When the pH is high OCl^- is a dominant species in water and when pH is decreased from 9 to 8, the concentration of OCl^- decreases sharply and HOCl concentration is increased relatively. Around pH of 7 and lower than 7, Cl_2 starts to produce. It is evident that ClO_2 is a weaker oxidant as compared to HOCl and pH is maintained at 6–7 at RO_1 [41]. The pH plays an important role in the reduction of inorganic scale precipitation. To control the pH, adjust the pH of the effluent from the municipal reclaimed water treatment system to be between 6 and 7. The silt density index (SDI) is basically applied to determine the fouling potential of particulate matters present at the inlet of RO and NF. Alhadidi et al. [42] proposed that the reliability of SDI_{15} is strongly questioned. He investigated the effect of membrane properties on the value of SDI_{15} and concluded that the SDI_{15} is not a reliable test. But the measurement of SDI_{15} is a general practice carried out in RO systems and SDI_{15} is 1.53, always maintained lower than 3.

The removal efficiency of the remaining COD and NH_3–N by the reverse osmosis system reaches almost 100%. Oxidation–reduction potential has several applications. It indicates the disinfection potential of a system, a high value of ORP implies the presence of an effective disinfection environment and lower microorganism count, to provide the estimated dosage of disinfectant and manipulate the oxidant or reductant dosing in water treatment systems [43]. It implies that ORP is a critical parameter that needs continuous monitoring and RO performance also depends on ORP. The ORP has maintained lower than 200 mV at the

RO system. Calcium carbonate and barium sulfate have very low solubility limits and show the specific scaling potential of the membrane surface. Along the length of the RO membrane, the concentration of salts increased on the concentrate side of the membrane. It is due to the removal of water from the permeate side. When the saturation limit exceeds then precipitation occurs [44]. Sweity et al. [45] investigated the effect of antiscalants on biofilm production on RO membrane. He concluded that polyacrylate-based antiscalants can alter the physico-chemical properties of RO membrane increasing the attachment of bio-material to the membrane at initial stages. He further described that polyphosphonate-based antiscalants act as a source of nutrients for microorganism. So, a controlled amount of antiscalant is dosed in RO_1. A specified quantity of 3 mg/L of antiscalant is dosed at RO_1 inlet. The concentration of HCO^{3-} ions in the municipal reclaimed water has reached 272.75 mg/L. At RO_2, the equilibrium of bicarbonate and carbonate ions is achieved. At pH of 8.3 HCO^{3-} ions are converted into CO_3^{2-} ions that resulted in carbonate precipitation removed by RO_2. To qualify as demineralized water and reduce the load of CEDI, soluble carbon dioxide is removed at RO_2 by adjusting the pH. The 5% sodium hydroxide (NaOH) solution is injected at the inlet of RO_2 to maintain the water pH around 8.3. Recovery rate (RR) is an important operation parameter of RO. The TMP is kept in specified range by adjusting the RR. Song et al. [46] investigated the performance limitations of full-scale RO membrane and concluded that permeate flux and TMP rises simultaneously. The RR of the RO_1 is 75% lower than the RO_2 85% because the contaminant level is higher at RO_1 and saturation of salts is avoided at concentrate water side by decreasing the RR. The RO_1 permeate water contains a smaller amount of TDS. It implies that solubility limit of dissolved salts here is the higher result in a higher RR can be achieved. The operational data of RO from August to October shown in Fig. 10. According to statistics, the effect of increased rainfall on the quality of municipal reclaimed water is the main reason for fluctuations in the conductivity of the RO system. It is found that the average desalination rate of the RO_1 system and RO_2 system is about 98.2% and 98.3%, respectively. The flux is maximum at the initial stage when a new device is put into operation and inlet pressure of RO reaches to equilibrium. After the continuous operation, the final equilibrium is achieved after ions and dosing chemicals in water are stabilized. The RO_2 system greatly reduced the ions in water. In order to further remove residual ions in the water, the water RR of RO_2 is increased and the operating parameters are higher than RO_1. The pressure drops between the first inlet side and the concentrated side, the pressure drop between the second inlet sides and the concentrated side of RO_2 remains within the allowable range. A recovery chemical cleaning is performed every 6 months to increase the service life and reduce the pressure drop between the inlet sides and the concentrated side of the RO membrane.

3.2.3. Continuous electrodeionization (CEDI/EDI) system

The separation process combining ion exchange resin with ion-exchange membranes is a hybrid process known as EDI. EDI is an effective environmental friendly process to remove weakly ionized species that RO cannot remove from water. The operating efficiency of EDI is determined by current strength, flow velocity in permeate, and concentrate water side compartments, temperature, and TDS of water. The resin is filled with ion-depleting compartments and helps in the transport of ions and takes part in electro-chemical reactions such as dissociating water into H^+ and OH^- ions [47].

Wood et al. [48] also discussed the feedwater requirements of EDI. He categorized feedwater requirements as temperature, TDS, and CO_2 that can affect the performance of EDI and all other parameters that can damage the EDI module like high pressure, organics, and foulants. He also explained that the quality of water produced by EDI is equivalent to that of mixed-bed deionizer and used as source of water supply to boilers for steam generation. A Siemens (USA) ionpure LX-Z was under observation during this study. The pressure of the freshwater chamber of the CEDI module is controlled to be higher than the pressure of the concentrated water chamber by 0–1.0 bar. When the required pressure on freshwater side and concentrate water side is achieved then CEDI system is energized. The control current is 2.0–3.0 A and RR of CEDI

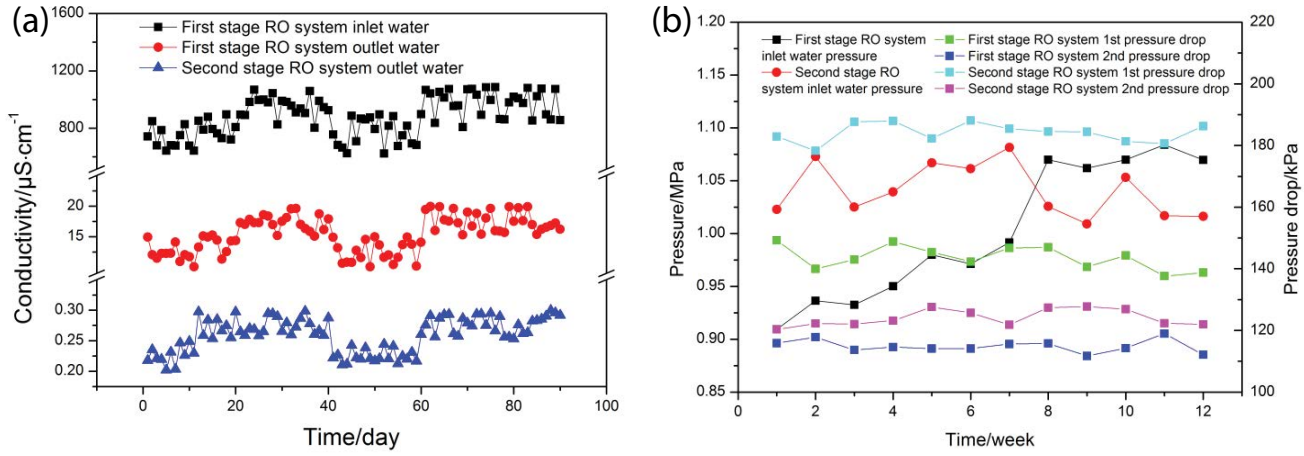

Fig. 10. RO system operation: (a) water conductivity in RO systems and (b) pressure and the pressure drop in RO system.

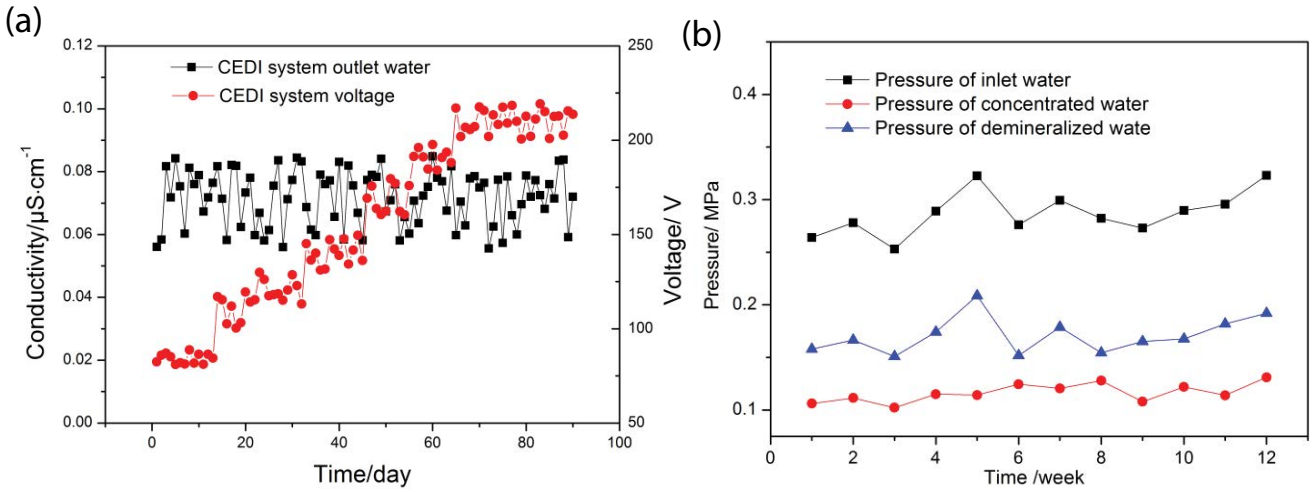

Fig. 11. CEDI system operation: (a) relation of conductivity and voltage with time and (b) behavior of pressure of inlet, concentrated side, and DM water with time.

system is set to 90%. The CEDI system is flushed first and then demineralize water is produced and stored in demineralize water tank. The operation data of the EDI system from August to October is shown in Fig. 11. As the resin layer in the module slowly reaches the regeneration balance with the water production process, then the module voltage increases to 200 V with the operating module resistance in the CEDI system. The conductivity of treated water is affected by change in conductivity of inlet water and the exchange capacity of resin in CEDI device. The conductivity of water during operation remains around 0.10 μS/cm which meets the requirements of the power plant. When operational parameters remain in range then conductivity of 0.08 μS/cm or even lower can be achieved.

3.3. Economic analysis of unit operation

The thermal power plant uses raw water as their necessary means of production is Q each year. The total investment of all the water treatment facilities is E (million USD). According to the price issued by the local government, the price of surface water from south to north water transfer project, the municipal reclaimed water, and the operating cost of the system is approximately P_1, P_2, and P_3, respectively. The direct economic benefit annual savings for the thermal power plant is W (million USD). There is no acid–base wastewater drainage that needs to be treated. There is also no need to buy acid and alkali to the resin regeneration system. In addition, the indirect and social benefits of using municipal reclaimed water are not included. The payback period of the project investment is T (months).

Eqs. (4) and (5) present the models for the annual savings for the thermal power plant and the payback period of the project investment:

$$W = Q(P_1 - P_2 - P_3) \times 10^{-6} \tag{4}$$

$$T = \frac{12E}{W} \tag{5}$$

Include, Q = 11.06 × 10^6 m^3, E = 20.84 million USD, P_1 = 1.34 USD/m^3, P_2 = 0.54 USD/m^3, and P_3 = 0.11 USD/m^3. After calculation, W = 7.63 million USD. The payback period of the project investment is 33 months.

4. Conclusion

This study describes a successful case of using municipal recycled wastewater in the thermal power plant. It is complicated to use municipal reclaimed water because of water quality issues. The combination of lime coagulation and full-membrane water treatment methods successfully solved this problem.

- The optimal conditions are obtained by the response surface method and combine with the actual situation. In conclusion, the PFS dosage (30 mg/L), the NaClO dosage (4.5 mg/L), the stirring rate (300 rpm), temperature (20°C), pH of flocculant area adjusted by adding lime (10.1), inlet flow (800 t/h), and pH of effluent adjusted by adding H_2SO_4 (6.5). Under these conditions, COD and NH_3–N removal rate is 84.72%, 88.25%, and 87.74%, respectively.
- After the outlet water from the coagulant treatment system passes through the DMF-UF system, the turbidity decreases to below 0.1 NTU and the SDI_{15} is 1.53. Because the pore size of the UF is not enough to trap NH_3–N and small organic matter, the removal rate of COD and NH_3–N is only 4.7% and 10.3% through the DMF-UF system. The removal rate of the remaining COD and NH_3–N by the reverse osmosis system reach almost 100%. The conductance of water reduced to 14.3 μS/cm after RO_1. By adjusted the pH of RO_2 inflow, the conductance of effluent decreased to 0.3 μS/cm after RO_2. Then decreased to 0.08 μS/cm after CEDI. Meet the thermal power plant boiler make-up water requirements.
- The power plant uses municipal reclaimed water through coagulation and full-membrane technique, 11.06 × 10^6 m^3 of surface water from south to north water project transfer is saved each year. The annual savings for the thermal

power plant is about 7.63 million USD. The payback period of the project investment is 33 months.

References

[1] UN. GA, Transforming Our World: The 2030 Agenda for Sustainable Development, Division for Sustainable Development Goals, New York, NY, 2016.

[2] Ministry of Water Resources People's Republic of China, China Water Resources Bulletin, 2017, China Water Power Press, Beijing, 2018.

[3] F. Huang, T. Du, S. Wang, X. Mei, D. Gong, Y. Chen, S. Kang, Current situation and future security of agricultural water resources in north China, Strategic Study Chin. Acad. Eng., 21 (2019) 28–37.

[4] Housing and Urban-Rural Development People's Republic of China, Statistical bulletin on urban and rural construction 2016, Urban Rural Dev., 17 (2017) 38–43 (in Chinese).

[5] R. Wen, B. Banik, R.K. Pathak, A. Kumar, N. Kolishetti, S. Dhar, Nanotechnology inspired tools for mitochondrial dysfunction related diseases, Adv. Drug Deliv. Rev., 99 (2016) 52–69.

[6] Ministry of Ecology and Environment, Action Plan for Prevention and Control of Water Pollution, People's Publishing House, Beijing, 2015.

[7] A. Gu, F. Teng, Y. Wang, China energy-water nexus: assessing the water-saving synergy effects of energy-saving policies during the eleventh Five-year Plan, Energy Conserv. Manage., 85 (2014) 630–637.

[8] H.Z. Song, Study on the Distribution Characteristics and the Exploration and Development Prospect of Coal Resource of China, China University of Geosciences, Beijing, 2013.

[9] S.G. Yin, Z.F. Ma, P. Huang, Q.Y. Wu, Research on the spatial and temporal distribution pattern of water resources utilization in China, J. Cent. China Normal Univ., 51 (2017) 841–848 (in Chinese).

[10] Y.S. Wei, L.B. Zheng, C. Zhang, D.W. Yu, Y.W. Wang, J.X. Zheng, Z.G. Yue, G. Wang, Progress of application and research of advanced treatment technologies for reclaimed water reuse in thermal power generation plant in China, Water Resour. Prot., 34 (2018) 1–16 (in Chinese).

[11] C.B. Jiang, Research on Water Treatment Technology of Reclaimed Water Reused in Thermal Power Plant, Southwest Jiaotong University, Chengdu, 2015 (in Chinese).

[12] X. Gao, Y. Zhao, S. Lu, Q. Chen, T. An, X. Han, L. Zhuo, Impact of coal power production on sustainable water resources management in the coal-fired power energy bases of northern China, Appl. Energy, 250 (2019) 821–833.

[13] S.Y. Sun, Y.L. Li, D.Y. Guo, L.L. Yu, H. Li, Analysis of water supply status and water resources balance in Hebei Province, Water Resour. Plan. Des., 10 (2018) 62–67 (in Chinese).

[14] H.Y. Zhang, L.T. Zhao, D.B. Liu, J. Wang, X.J. Zhang, C. Chen, Early period corrosion and scaling characteristics of ductile iron pipe for ground water supply with sodium hypochlorite disinfection, Water Res., 176 (2020) 1–10, doi: 10.1016/j.watres.2020.115742.

[15] A.R. Rakitin, V.I. Kichigin, Electrochemical study of calcium carbonate deposition on iron. Effect of the anion, Electrochim. Acta, 54 (2009) 2647–2654.

[16] C. Chen, L.H. Jiang, M.Z. Guo, P. Xu, L. Chen, J. Zha, Effect of sulfate ions on corrosion of reinforced steel treated by DNA corrosion inhibitor in simulated concrete pore solution, Constr. Build. Mater., 228 (2019) 1–8, doi: 10.1016/j.conbuildmat.2019.116752.

[17] S. Jain, B. Pradhan, Fresh, mechanical, and corrosion performance of self-compacting concrete in the presence of chloride ions, Constr. Build. Mater., 247 (2020) 1–16, doi: 10.1016/j.conbuildmat.2020.118517.

[18] D. Georgiou, V. Liliopoulos, A. Aivasidis, Investigation of an integrated treatment technique for anaerobically digested animal manure: lime reaction and settling, ammonia stripping and neutralization by biogas scrubbing, Bioresour. Technol. Rep., 5 (2019) 127–133.

[19] I.M. Ismail, A.S. Fawzy, N.M. Abdel-Monem, M.H. Mahmoud, M.A. El-Halwany, Combined coagulation flocculation pre treatment unit for municipal wastewater, J. Adv. Res., 3 (2012) 331–336.

[20] D. Căilean, G. Barjoveanu, C. Teodosiu, L. Pintilie, I.G. Dăscălescu, C. Păduraru, Technical performances of ultrafiltration applied to municipal wastewater treatment plant effluents, Desal. Water Treat., 56 (2015) 1476–1488.

[21] Q. Yang, W.I. Whiting, R. Dettori, A membrane with ion fluxes responsive to temperature, pH and voltage, J. Membr. Sci., 578 (2019) 10–15.

[22] N.F. Gray, S.L. Percival, M.V. Yates, D. Williams, Microbiology of Waterborne Diseases, 2nd ed., Elsevier Science Publishing Co., Inc., United States, 2014.

[23] M. Achak, F. Elayadi, W. Boumya, Chemical coagulation/flocculation processes for removal of phenolic compounds from olive mill wastewater: a comprehensive review, Am. J. Appl. Sci., 16 (2019) 59–91.

[24] C.S. Lee, J. Robinson, M.F. Chong, A review on application of flocculants in wastewater treatment, Process Saf. Environ. Prot., 92 (2014) 489–508.

[25] K.E. Lee, N. Morad, T.T. Teng, B.T. Poh, Development, characterization and the application of hybrid materials in coagulation/flocculation of wastewater: a review, Chem. Eng. J., 203 (2012) 370–386.

[26] X.S. Yi, W.X. Shi, S.L. Yu, N. Sun, L.M. Jin, S. Wang, B. Zhang, C. Ma, L.P. Sun, Comparative study of anion polyacrylamide (APAM) adsorption-related fouling of a PVDF UF membrane and a modified PVDF UF membrane, Desalination, 286 (2012) 254–262.

[27] M.F. Chong, Direct Flocculation Process for Wastewater Treatment, S. Sharma, R. Sanghi, Eds., Advances in Water Treatment and Pollution Prevention, Springer, Dordrecht, 2012, pp. 201–230.

[28] J.Q. Jiang, N.J.D. Graham, Observations of the comparative hydrolysis/precipitation behaviour of polyferric sulphate and ferric sulphate, Water Res., 32 (1998) 930–935.

[29] W.P. Cheng, Hydrolysis characteristic of polyferric sulfate coagulant and its optimal condition of preparation, Colloids Surf., A, 182 (2001) 57–63.

[30] J.L. Cui, C.Y. Jing, D.S. Che, J.F. Zhang, S.X. Duan, Groundwater arsenic removal by coagulation using ferric(III) sulfate and polyferric sulfate: a comparative and mechanistic study, J. Environ. Sci., 32 (2015) 42–53.

[31] A.M. Diab, H.E. Elyamany, M. Abd Elmoaty, M.M. Sreh, Effect of nanomaterials additives on performance of concrete resistance against magnesium sulfate and acids, Constr. Build. Mater., 210 (2019) 210–231.

[32] J.T. Miller, H.J. Martin, E. Cudjoe, Comparison of the effects of a sulfuric acid environment on traditionally manufactured and additive manufactured stainless steel 316L alloy, Addit. Manuf., 23 (2018) 272–286.

[33] A.I. Hermoso-Diaz, A.E. Foroozan, J.P. Flores-De los Rios, L.L. Landeros-Martinez, J. Porcayo-Calderon, J.G. Gonzalez-Rodriguez, Electrochemical and quantum chemical assessment of linoleic acid as a corrosion inhibitor for carbon steel in sulfuric acid solution, J. Mol. Struct., 1197 (2019) 535–546.

[34] P. Ncube, M. Pidou, P. Jarvis, The impact of filter bed depth and solids loading using a multimedia filter, Sep. Sci. Technol., 53 (2018) 2249–2258.

[35] A. Zouboulis, G. Traskas, P. Samaras, Comparison of single and dual media filtration in a full-scale drinking water treatment plant, Desalination, 213 (2007) 334–342.

[36] M. Hong, Study on factors affecting separation of xylose from glucose by nanofiltration using composite membrane developed from triethanolamine (TEOA) and trimesoyl chloride (TMC), J. Eng. Sci. Technol., 10 (2014) 92–100.

[37] H. Wu, X. Niu, J. Yang, C. Wang, M. Lu, Retentions of bisphenol A and norfloxacin by three different ultrafiltration membranes in regard to drinking water treatment, Chem. Eng. J., 294 (2016) 410–416.

[38] R. Ramli, N. Bolong, Effects of pressure and temperature on ultrafiltration hollow fiber membrane in mobile water treatment system, J. Eng. Sci. Technol., 11 (2016) 1031–1040.
[39] S.H. Maruf, D.U. Ahn, J. Pellegrino, J.P. Killgore, A.R. Greenberg, Y. Ding, Correlation between barrier layer Tg and a thin-film composite polyamide membrane's performance: effect of chlorine treatment, J. Membr. Sci., 405 (2012) 167–175.
[40] W.J. Lau, A.F. Ismail, N. Misdan, M.A. Kassim, A recent progress in thin film composite membrane: a review, Desalination, 287 (2012) 190–199.
[41] R. Verbeke, V. Gómez, I.F.J. Vankelecom, Chlorine-resistance of RO (RO) polyamide membranes, Prog. Polym. Sci., 72 (2017) 1–15.
[42] A. Alhadidi, A.J.B. Kemperman, J.C. Schippers, M. Wessling, W.G.J. van der Meer, The influence of membrane properties on the Silt Density Index, J. Membr. Sci., 384 (2011) 205–218.
[43] R.J. Xie, E.K. Tan, A.N. Puah, Oxidation-reduction potential in saline water reverse osmosis membrane desalination and its potential use for system control, Desal. Water Treat., 3 (2009) 193–203.
[44] M.K. Shahid, M. Pyo, Y.G. Choi, The operation of reverse osmosis system with CO_2 as a scale inhibitor: a study on operational behavior and membrane morphology, Desalination, 426 (2018) 11–20.
[45] A. Sweity, T.R. Zere, I. David, S. Bason, Y. Oren, Z. Ronen, M. Herzberg, Side effects of antiscalants on biofouling of reverse osmosis membranes in brackish water desalination, J. Membr. Sci., 481 (2015) 172–187.
[46] L. Song, J.Y. Hu, S.L. Ong, W.J. Ng, M. Elimelech, M. Wilf, Performance limitation of the full-scale reverse osmosis process, J. Membr. Sci., 214 (2003) 239–244.
[47] Ö. Arar, Ü. Yüksel, N. Kabay, M. Yüksel, Various applications of electrodeionization (EDI) method for water treatment—a short review, Desalination, 342 (2014) 16–22.
[48] J. Wood, J. Gifford, J. Arba, M. Shaw, Production of ultrapure water by continuous electrodeionization, Desalination, 250 (2010) 973–976.